A HYBRID DETECTOR SYSTEM FOR 100-GeV STRONG INTERACTIONS*

T. Fields
Argonne National Laboratory

A. Roberts
National Accelerator Laboratory

D. Sinclair and J. Vander Velde
University of Michigan

and

T. G. Walker
Rutherford High Energy Laboratory

June 29, 1968

Introduction

The ability to study the details of multiparticle final states at 100 GeV will hopefully be at least as fruitful as it has proven to be at energies less than 10 GeV. Therefore, we have considered the design of a visual detector system which will be capable of analyzing complex events at 100 GeV with an accuracy and solid angle comparable to that of present bubble chambers at 10 GeV. This capability can be reached quite fully and economically by using a hybrid detector which will possess many of the advantages of both bubble chambers and spark chambers, we have concluded. The composite system should consequently offer important advantages in comparison to present-day bubble chambers, and it should also compare favorably with very large hydrogen bubble

*This is a highly condensed version of NAL Summer Study Report A. 3-68-12.

chambers for 100-GeV strong-interaction experiments. The extent to which this (or any visual device) can compete with an all-electronic detection system is very experiment-dependent, of course, but there are many reasons to expect that visual devices will continue to have essential roles in strong-interaction physics.

The practicability of the system which we discuss follows from the fact that particles tend to be produced with low transverse momenta. Thus particles with high momentum in the center-of-mass frame tend to come out in the lab in two jets. The slow jet contains particles associated with the target vertex which tend to have low momenta and large angles and therefore are suitable for accurate analysis in a small bubble chamber. The fast jet contains particles associated with the beam vertex and these tend to have very high momenta and very small angles, suitable for analysis in a large spark chamber magnetic spectrometer.

Description

The system as shown in Fig. 1 consists of the following major elements:

1. A one-meter rapid cycling hydrogen bubble chamber in a 40kG field. This measures particles of momentum $\leq$ 5 GeV/c at all angles. Table I gives general information on the bubble chamber.

2. An intermediate spectrometer, the magnet of which provides 60 kG-m. This covers the range $5 < P < 20$ GeV/c and angles up to 9°. See Table II and Fig. 2.

3. A high-momentum spectrometer with a 160 kG-m magnet which includes angles up to 0.0375 rad = 2.1°. See Table III and Fig. 1.

4. (Optional) A set of large heavy plate spark chambers located downstream of the spectrometer systems to detect and thus measure the direction of gamma rays from the decay of fast forward π^{o}'s, etc.

These elements (except for the heavy plate chambers) are designed to provide momentum measurements to an accuracy of $dP \leq 0.1$ GeV/c and angle measurements to an accuracy of $Pd\theta < 0.1$ GeV/c, for the momentum and angular ranges given. Such criteria should provide an accuracy of kinematic fitting as good as is now in everyday use at ~ 5 GeV.

It is likely that a negligible fraction of particles will fall outside of these momentum and angular ranges. Figure 3 shows the limits of these ranges for the various elements of the system on a c. m. momentum plot for 100-GeV incident momentum, together with the secondary particle distribution given by Fiorini.[1] The boundaries shown are ones within which the above accuracy criteria are met. Even the rare tracks outside these boundaries can be measured to reasonable accuracy, of course.

A simple trigger signal, namely, the failure of one of the beam tracks to traverse the system without momentum loss, would be very useful for many purposes. Using this trigger to flash the bubble chamber light, to fire the spark chambers, and to turn off the incident beam will result in just one interaction in the bubble chamber, and one set of

outgoing tracks in the spark chambers. This mode should yield 5-10 unbiased evnets per machine pulse, with about half of these events occurring in a good fiducial region of the bubble chamber. Additional trigger requirements on either the incoming or outgoing particles could be useful for many experiments, and would often be used to tag the photographs.

Operating in an unselective triggering mode, this system could easily yield 10 or 20 million events per year, quite comparable to what a large conventional HBC can give. Fast cycling and the use of about 10 beam tracks per picture are, of course, the means by which the small chamber hybrid system becomes competitive in rate. To achieve freedom from unwanted secondary interactions, the downstream spark chamber part of the system allows a much lower density than that of liquid hydrogen, deuterium, or neon.

To compare the accuracy of this system with that of large bubble chambers, we have considered the following two cases: NAL 25-foot HBC, B = 40 kG, spatial error = 0.6 mm, and ANL 12-foot HBC, B = 20 kG, spatial error = 0.3 mm. With these parameters, and neglecting secondary interactions, the momenta at which these large bubble chambers are comparable in accuracy to our 100-GeV hybrid system are 18 and 9 GeV/c, respectively.

Discussion

The values which we have chosen for the various parameters of this system are meant to be ones whose feasibility is clear at present.

They are surely not optimum values, so that a considerable effort in design and development should precede any serious planning for a system like this. Equally important, a hybrid system of this general type could do some interesting experiments at present energies and simultaneously yield some real operating experience.

Costwise, the 100-GeV hybrid system would probably represent about half the investment of a 25-foot HBC, but would not be of any use for neutrino experiments. Many of the elements of the hybrid system (e.g., high field, large aperture magnets) will be needed at NAL in any case. The flexibility which follows from the modular nature of the hybrid system would be advantageous in many ways. For example, the major improvements which continue to occur in the technologies of bubble chambers, spark chambers, and magnets could be regularly and economically incorporated in the system.

Acknowledgments

Most of this report is a direct outgrowth of detector system studies which have appeared in Berkeley and ECFA study reports. We have also profited from discussions with many of our colleagues at several institutions. The recent experience of the Wisconsin groups with the PPA rapid-cycling bubble chamber has been a further stimulus to this work.

REFERENCE

[1] Utilization Studies for 300 GeV Synchrotron, CERN/ECFA 67/16, Vol. I, p. 299.

Table I. Bubble-Chamber Parameters.

Size - 1 m diameter × 0.5 m deep

Field - 40 kG (superconducting magnet)

Optics - conventional

Spatial Precision - 80 μm

Film - 35 mm

Rate - 5-10 expansions/flat top

Beam Windows - $2 \times 15\ cm^2$ entrance, $25 \times 50\ cm^2$ exit; total thickness $\leq$ 0.5 rad length and 0.1 coll. length

Gap Between Coils - 50 cm

Table II. 5-20 GeV/c Spectrometer.

Magnet - LWH = $2 \times 2.6 \times 1.6\ m^3$

Field - 30 kG (superconducting magnet)

Angular Acceptance - ± 150 mrad

Wide Gap Chamber (4) - Smallest $0.4 \times 0.4\ m^2$, largest $2.0 \times 2.4\ m^2$

Spatial Precision - 0.2 mm

Total Chamber Thickness - 0.01 rad length

Table III. 20-100 GeV/c Spectrometer.

Magnet - LWH = $4 \times 1 \times 1.5\,m^3$
Field - 40 kG (superconducting magnet)
Angular Acceptance - ± 40 mrad
Wide Gap Chambers (3) - Smallest $0.6 \times 1.2\,m^2$, largest $4.6 \times 2.2\,m^2$
Spatial Precision - 0.2 mm
Total Chamber Thickness - 0.01 rad length

FIGURE CAPTIONS

Fig. 1. Hybrid spectrometer for the analysis of high-energy interactions; it includes the fast-cycling bubble chamber (left) and two spectrometers using spark chambers for momentum determination. Gamma-ray chambers detect fast neutral pions. Angles shown are production angles in radians, momenta in BeV/c.

Fig. 2. Detailed view of intermediate momentum spectrometer.

Fig. 3. Peyrou plot of the momentum distribution of particles generated by a Monte Carlo program. The heavy line indicated the limits within which particles will be detected in the system specified above. The system loses very few particles.

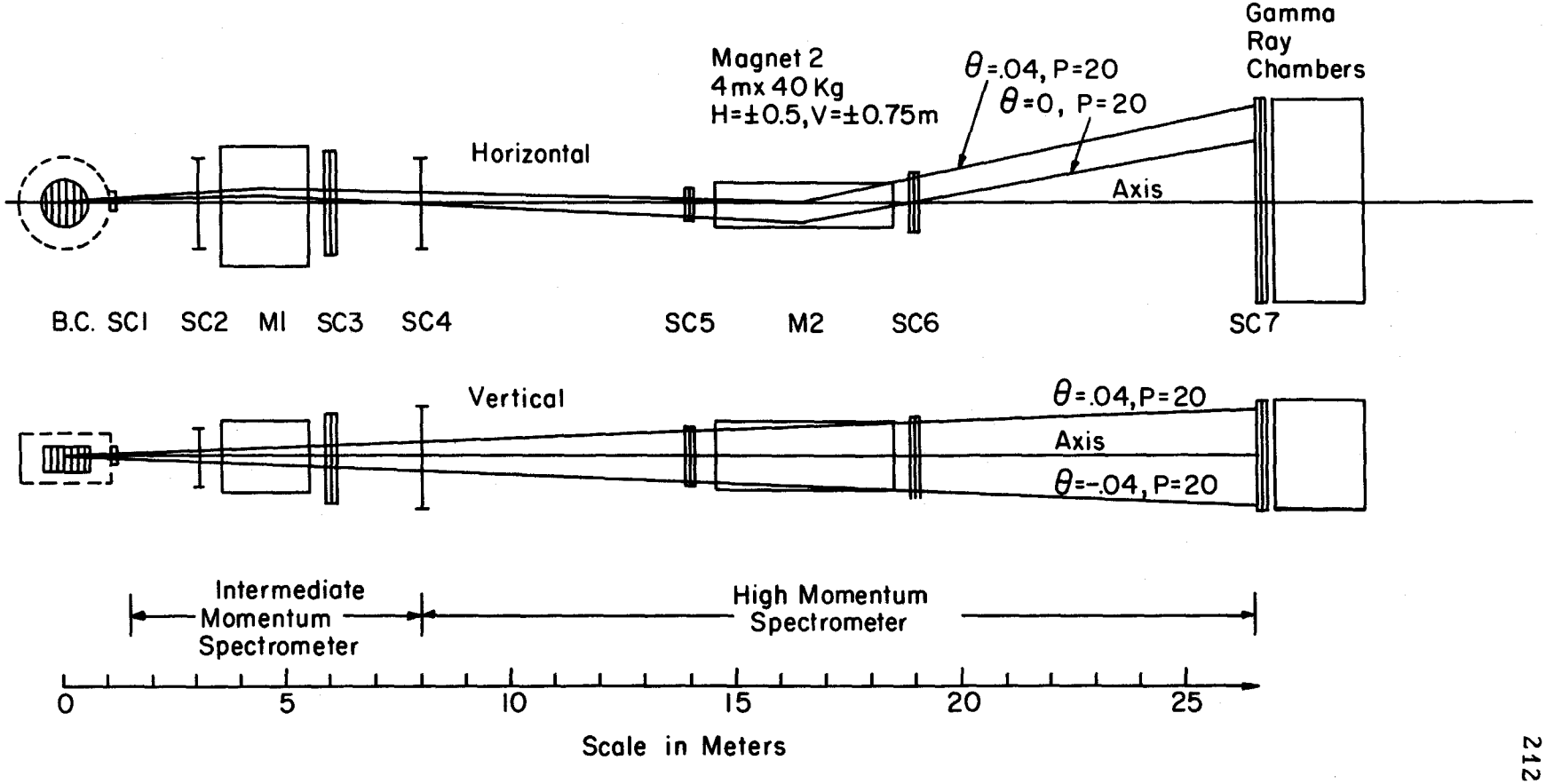

Fig. 1

TM-104
2122

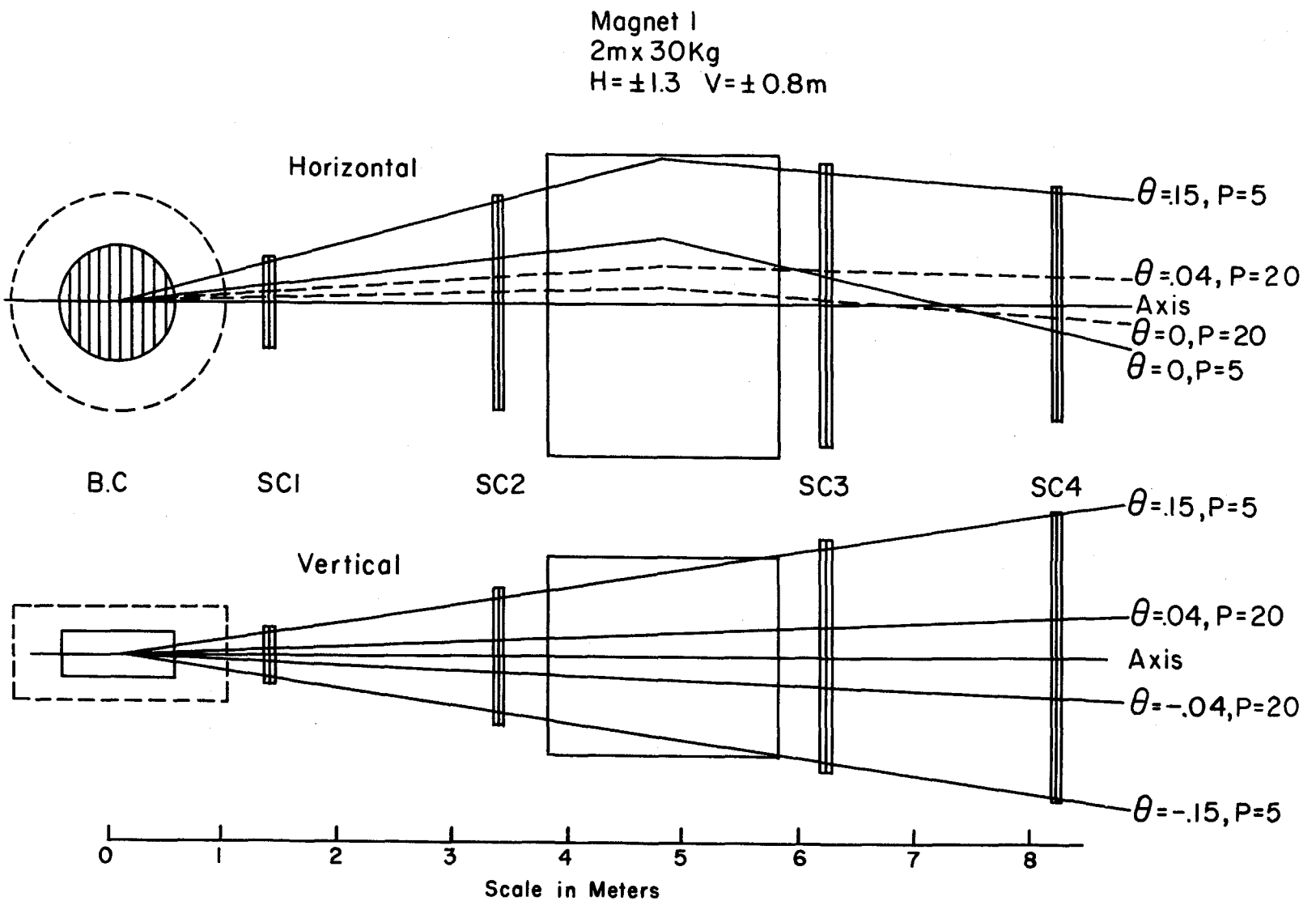

Fig. 2

TM-104
2122

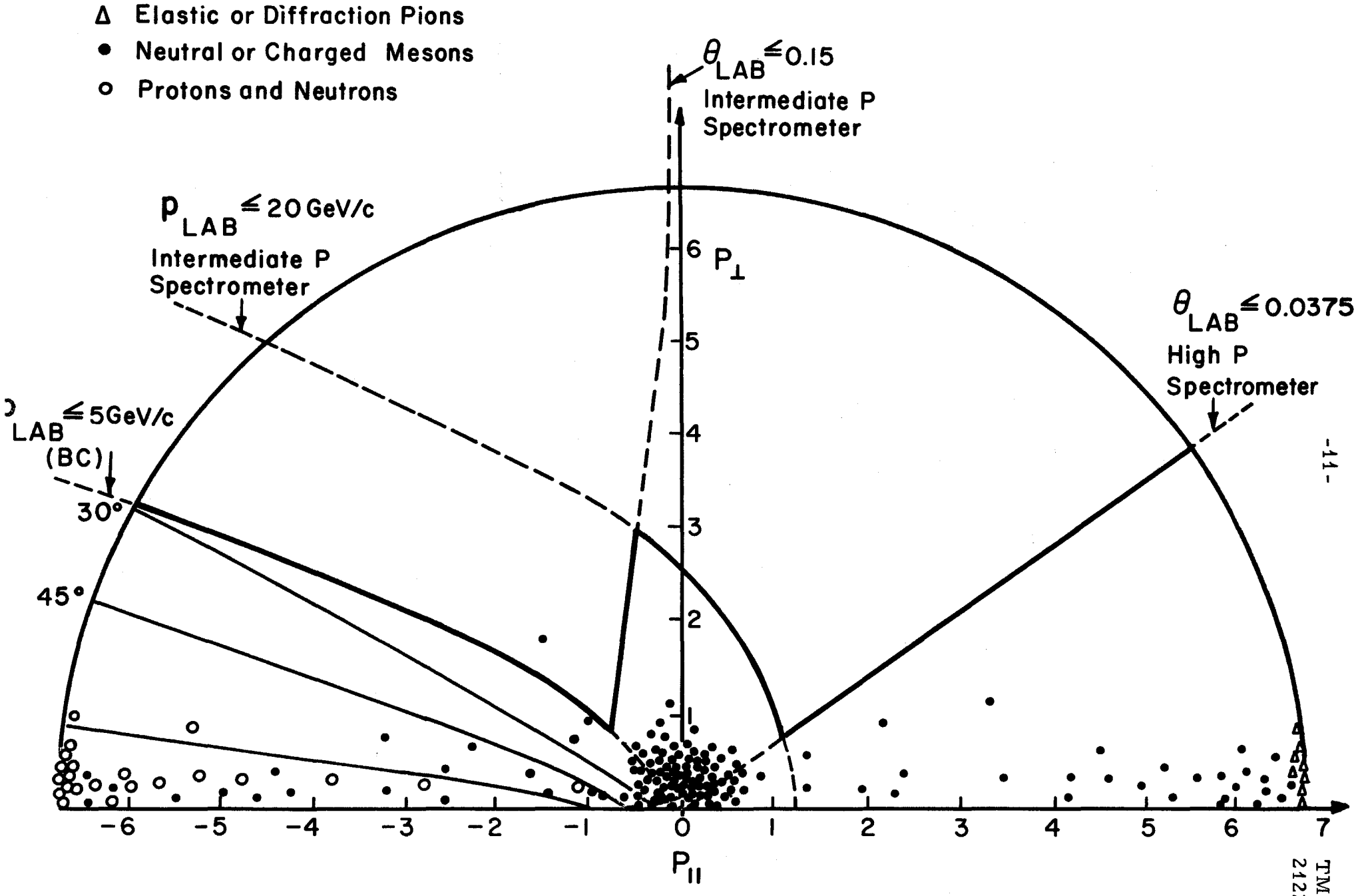

Fig. 3

TM-104
2122